JOURNAL OF GEOPHYSICAL RESEARCH, VOL. 103, NO. D13, PAGES 16,397–16,409, JULY 20, 1998

Particle production in the remote marine atmosphere: Cloud outflow and subsidence during ACE 1

A. D. Clarke and J. L. Varner

School of Ocean and Earth Science and Technology, University of Hawaii, Honolulu

F. Eisele,[1] R. L Mauldin, and D. Tanner

Atmospheric Chemistry Division, National Center for Atmospheric Research, Boulder, Colorado

M. Litchy

School of Ocean and Earth Science and Technology, University of Hawaii, Honolulu

Abstract. During November and December 1995 the First Aerosol Characterization Experiment (ACE 1) was undertaken as part of the International Global Atmospheric Chemistry (IGAC) Program. A key objective of the aircraft component of this experiment included the identification of source regions for new particles in the remote marine atmosphere. No evidence was found for particle production in the marine boundary layer (MBL), but extensive observations of enhanced layers of "new" particles were found in the free troposphere (FT). These layers were generally found at altitudes that corresponded to nearby cloud top heights and exhibited concentrations that exceeded MBL air by about 1000 to 10,000 cm^{-3}. Many layers were also associated with enhanced concentrations of water vapor and sulfuric acid. Focused cloud experiments demonstrated that these particles were recently formed and originated in the outflow region of clouds preferentially after late morning when photochemical processes had become sufficiently active. The production and growth of these particles were rapid, and they appeared to evolve and merge with a background nuclei spectra on the scale of hours to a day. These measurements in midlatitude postfrontal air undergoing shallow convection indicated that particles were produced in the trailing cloud outflow region as low as 2 km altitude and that the base of this layer extended down to the inversion in the region of postfrontal subsidence. Other ACE 1 measurements made in transit near equatorial convection also revealed small nuclei aloft at altitudes up to 6 km and a trend in decreasing concentrations, in conjunction with steadily increasing size, during descent toward the surface. The concentration and size distributions in this these regions indicate that significant numbers of new nuclei are formed aloft in various cloud outflow regions and that they can provide a source for the MBL aerosol via subsidence. This nucleation appears to be favored when existing surface areas approach or drop below about 5-10 μm^2 cm^{-3}.

1. Background

The origin of condensation nuclei (CN) in the remote marine atmosphere has been an objective of numerous research programs for the past two decades. Observations of substantial emissions of sulfur in the form of dimethyl sulfide (DMS) from the ocean surface prompted suggestions that its oxidation products could provide a natural source for marine aerosol sulfate [*Bonsang et al.*, 1980; *Andreae and Raemdonck*, 1983]. Uncertainties over the nature of the conversion process prompted speculation that new particle formation might be initiated via gas to particle conversion and that these particles might have climatological significance through their influence on the abundance of CN and of cloud condensation nuclei (CCN) in the marine boundary layer (MBL) [*Charlson et al.*, 1987]. This interest provided impetus for various experiments that have attempted to demonstrate a link between DMS emissions, CN, and CCN in the MBL. However, unambiguous evidence for widespread new particle production in the MBL in response to elevated DMS has been difficult to demonstrate [*Bates et al.*, 1989], although some examples exist [*Hegg et al.*, 1990; *Covert et al.*, 1992; *Hoppel et al.*, 1994]. Other observations have tended to indicate that gas to particle (GPC) conversion in the MBL for regions with high DMS was more likely to result in growth of existing aerosol to larger sizes than the formation of new particles [*Clarke*, 1993; *Clarke et al.*, 1996; *Ayers et al.*, 1991].

Efforts to model nucleation of new particles in the MBL have been mixed in both the assumptions used and predicted results [*Shaw*, 1989; *Raes et al.*, 1993; *Hegg et al.*, 1990; *Kriedenweiss and Seinfeld*, 1988; *Russell et al.*, 1994; *Covert et al.*, 1992]. However, these papers and references therein clearly recognize that the vapor pressure of sulfuric acid and the presence of preexisting aerosol surface area are key parameters that determine whether nucleation of new particles will occur as opposed to condensation upon existing aerosol. Estimates of the maximum

[1]Also at GTRI, Georgia Institute of Technology, Atlanta.

Paper number 97JD02987.
0148-0227/98/97JD-02987$09.00

surface area conducive to nucleation for moderate to high sulfuric acid in the MBL suggest maximum values of about 10 μm^2 cm^{-3}. Typical measured MBL dry aerosol surface areas are about 20-100 μm^2 cm^{-3} [*Covert et al.*, 1996] and corresponding to about 50-200 μm^2 cm^{-3} "wet" at ~80% relative humidity in the MBL. Hence models predict that nucleation will not be favored in the MBL [*Raes*, 1995] unless aerosol surface area is markedly reduced through some removal process or by incursions of air with low surface area from aloft.

Recently, observations of extended high concentrations of small nuclei were made at higher altitudes in the FT near regions of deep convection [*Clarke*, 1993]. Highest concentrations were found associated with regions of lowest aerosol mass, and it was suggested that these nuclei were related to cloud process that scavenged surface-derived aerosol through precipitation but pumped aerosol precursors aloft to regions where low aerosol surface area favored new particle nucleation. Evidence for new particle formation near clouds has been observed recently [*Hegg et al.*, 1990; *Perry and Hobbs*, 1994; *Hoppel et al.*, 1994]. Nucleation consistent with these observations under similar conditions was also predicted by a FT model [*Raes et al.*, 1993], and application of this model to the convective equatorial region was used to predict the evolution and growth of this aerosol during subsidence to the MBL [*Raes*, 1995]. The resulting model-predicted size distribution above the MBL was consistent with that inferred for the observed entrainment and diurnal growth of aerosol measured in the equatorial Pacific [*Clarke et al.*, 1996]. Extensive MBL aerosol size-distribution measurements in the Pacific have also shown that regions of high pressure tended to reveal smaller nuclei than other regions, consistent with the notion of small nuclei subsiding from above [*Covert et al.*, 1996]. Exploring and testing this notion of aerosol nucleation in the free troposphere via cloud processes followed by growth and subsidence into the MBL was identified as a key objective of the First Aerosol Characterization Experiment (ACE 1) mission.

2. Instrumentation

The data reported here were collected as part of the ACE 1 experiment as part of the C-130 aircraft experiment [*Bates et al.*, this issue]. The instrumentation of direct relevance to these observations is described here. All data presented will be converted to concentrations at standard temperature and pressure (STP) so that comparisons between different altitudes can be made without concern over pressure corrections.

1. Laser optical particle counter (OPC) (Particle Measurement Systems LAS-X, Boulder, Colorado modified for 256 channel resolution) yields particle size distributions nominally from 0.14-7.0 μm diameter. Aerosol is preheated to 40, 150, and 300°C to infer aerosol composition from volatility [*Clarke*, 1991].

2. Condensation Nuclei (CN) counter (Thermal Systems Inc., Model 3760) counts total particle number from 0.015-3.0 μm, a second unit operated at 300°C counts "refractory CN" (RCN) remaining at 300°C. A third counter (TSI Model 3010), referred to below as our CN counter, was operated with a nominal lower size cut of 0.010 μm but tended to underestimate counts and required some flow and altitude corrections (5-10%) (R. J. Weber, personal correspondence, 1997).

3. Ultrafine Condensation Nucleus Counter (UCN) (Thermal Systems Inc., Model 3025) counts particles nominally between 0.003-3.0 μm. The difference between UCN and CN (TSI Model 3010) counter indicates recently formed particles present in 0.003-0.010 μm range and are referred to here as ultrafine (UF) particles. The nominal flow uncertainties in these instruments are estimated as about 5% each by the manufacturer, and the lower size cut of the TSI 3010 varied sometimes higher than the nominal 0.010 μm due to occasional large excursions in aircraft temperature near the instrument. As a result, this UF difference measurement can include particle counts for sizes greater than 0.010 μm, but the key results presented here will not be changed.

4. Radial Differential Mobility Analyzer (RDMA) is a small custom-built disc DMA [*Zhang et al.*, 1995] with particle sizing set at 0.01-0.25 μm using a TSI Model 3010 with 22°C saturator temperature difference for lowered detection limit and with thermal analysis similar to the OPC.

5. Ambient Aerosol Size is a composite ambient size distribution obtained with C-130 wing probe data from the FSSP-100 (0.2-47 μm), FSSP-300 (0.3-20 μm) (forward scattering spectrometer probes); PCASP (0.1-3.0 μm) and 260-X (10-620 μm) (all from Particle Measurement Systems, Boulder, Colorado) [*Baumgardner and Clarke*, this issue]. We will use the term FSSP here to refer to this composite data for the estimate of ambient aerosol surface area.

6. Integrating Nephelometer (Thermal Systems Incorporated, Model 3563) measures the light scattering coefficient and backscatter coefficient at three wavelengths [*Anderson et al.*, 1996]. It can often be used as a fast response but approximate index for variations in aerosol surface area.

7. H_2SO_4 gas phase sulfuric acid is measured using a selected ion chemical ionization mass spectrometer instrument [*Eisele and Tanner*, 1993] with specially designed inlet (Eisele et al., submitted). The instrument cycles through OH, H_2SO_4, and MSA measurements every 30 s with two 4 s measurements of H_2SO_4 in each 30 s period. This results in a minimum detection limit of about $1x10^5$ molecules cm^3 for each 30 s period. The response time of the instrument and inlet is much faster (subsecond) and is only limited by counting statistics at low concentrations.

Most of the particle instrumentation as deployed on the C-130 has been described elsewhere [*Clarke*, 1993; *Clarke et al.*, 1996] or in the references indicated above. The NCAR C-130 was equipped with the Community Aerosol Inlet (CAI) during ACE 1 so that our data and that of most aerosol investigators was sampled from the same inlet. A description and performance characterization of the CAI will be the subject of a future paper (B. Huebert, personal communication, 1997)

One new development used on ACE 1 is called a Lagged Aerosol Grab (LAG) chamber as an alternative to the more common but problem prone "BAG" sampler. Both systems collect an air sample over a 10-20 s period for subsequent (lagged) analysis. BAG samplers are usually fabricated from a conductive bladder inside a pressure vessel that provides for inflation and evacuation of the sample bag through a system of valves. Problems of leaks, loss of conductivity, incomplete evacuation, disrupted aerosol flow, etc. often compromise BAG sampler data but are largely eliminated in our LAG chamber design. Because RDMA observations are central to this paper, we describe the operation of the LAG chamber here. A LAG sampler was important for effective interpretation of RDMA data since many of the aerosol environments sampled revealed rapid variability in concentrations over the time period required for RDMA thermal scans (2-3 min).

The schematic for the LAG chamber is shown in Figure 1. It is a capped aluminum tube about 10 cm diameter and 130 cm long with an internal volume of about 10 L. Three way valves normally isolate the LAG chamber from the continuous flow line.

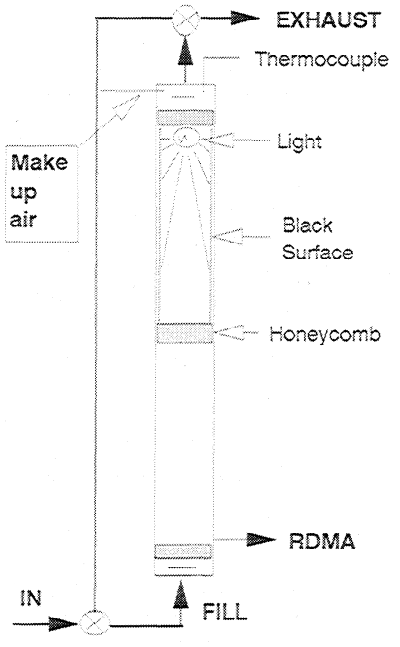

Figure 1. Schematic of key features of the LAG chamber used on the C-130 to obtain a grab sample for analysis with RDMA. See text for details.

When they are opened to collect a sample, the flow enters the bottom of the chamber and exits the top. A flow spreader and 3 mm diameter honeycomb aluminum (Hexcell Corp.) flow straightener are included at the base and at the top as well another near the middle that separates the chamber into upper and lower sections. These are intended to minimize large scale turbulence and help ensure "plug" flow through the chamber until the valves are closed to isolate the sample. The upper portion of the chamber has an incandescent light at the top and insulated black interior designed to result in a thermal gradient from the top toward the center of the chamber such that the air introduced into the chamber will be heated in a way that results in thermal stratification that suppresses vertical mixing.

The outlet to the RDMA is located at the base of the LAG chamber, and an inlet of makeup ambient air is located at the top of the thermally stratified upper chamber. For this experiment the introduction of ambient makeup air rather than filtered air was used since we presumed it would in general perturb upper chamber concentrations less. The low RDMA sample flow rate (less than 1.0 l m^{-1}) and the honeycomb chamber separation provides for low velocity "plug" flow downward in the chamber, while the incoming makeup air is heated by passage around the light at the top of the LAG chamber so that thermal stratification is preserved. The lower part of the chamber is about 6 L so that two complete RDMA thermal scans (6 scans total) can be completed in principle before air for the upper chamber reaches the RDMA outlet. During ACE 1, only three scans were completed before flushing the LAG chamber. The plug flow and excess volume was chosen to minimize the likelihood of diluted upper chamber air being sampled. Tests with filtered makeup air confirmed this performance. Having makeup air open to the inlet line also meant that the chamber always operated at external ambient pressure even during aircraft altitude changes. Tests of particle losses in the chamber under typical in situ operating conditions with a polydisperse aerosol revealed about a 15% net decrease over a 7 min period. By keeping the valves open the LAG chamber can also be operated in a continuous flush mode on occasions when that is desirable. When not being flushed, the bypass flow (Figure 1) maintained the same flow from the C-130 community inlet, ensuring isokinetic sampling conditions at all times.

3. Observations

ACE 1 aerosol nucleation missions aboard the C-130 had several primary objectives [*Bates et al.*, this issue], one of which was to characterize processes associated with nucleation in the troposphere and its relationship to the cycling of nuclei in the marine boundary layer. These included the identification of regions where recent nucleation was most evident, assessment of the possible role of clouds in promoting nucleation, investigation of the role of gas phase species in nucleation, testing the role of photochemistry in nucleation, and exploring the hypothesis that nucleation aloft followed by subsidence could be a means of providing the MBL with "new" particles. A full exposition of the details of nucleation events and the associated nucleation processes as they relate to our measurements are beyond the scope of this paper and will be the subject of a future paper(s). Rather, the intent here is to summarize some of the key observations that bear upon the above objectives and their implications. The emphasis will be on data for air masses representative of clean "background" air that is not perturbed by anthropogenic emissions.

The most rapid continuous aerosol measurements that characterize regions of recent nucleation are the measured differences between the UCN counter and the CN3010 counter which together provides the number of particles present in the 3-10 nm range, hereafter called UF particles. The more intermittent

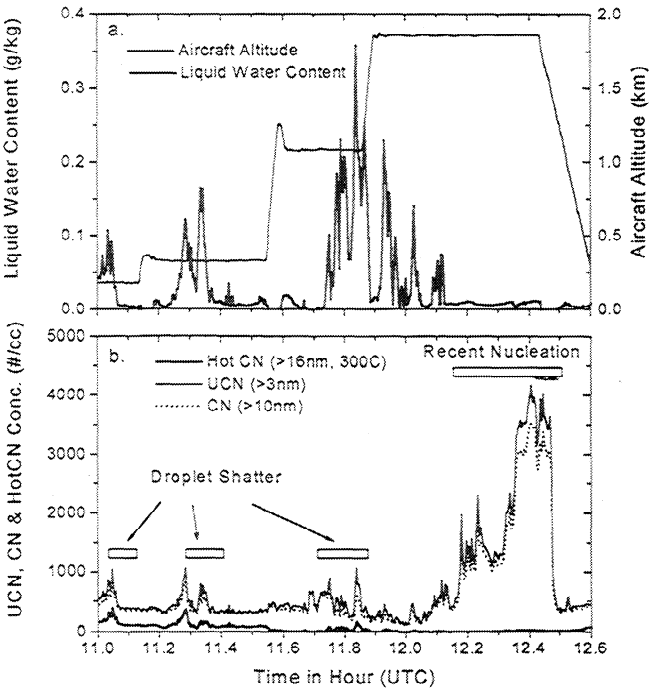

Figure 2. (a) Aircraft altitude and cloud liquid water content corresponding to droplet shatter and nuclei measurements. (b) Time series of UCN, CN, and hot CN for period when elevated nuclei counts were observed that included those from artifact droplet shatter and from true elevated nuclei events.

RDMA data provided essential information on the changes in the size distribution between 10 and 250 nm that reveal both the presence and later evolution of these "new" nuclei. Additional measurements that establish the size and early growth of these nuclei in the 3-7 nm range were also carried out aboard the C-130 (P. McMurry and R. Weber, University of Minnesota, 1997), but these will not be discussed here. Aerosol surface area under diverse conditions were determined from size distributions for larger aerosol obtained from the inboard "dry" OPC and the wing mounted "wet" aerosol FSSP probes. Of the various gas phase measurements aboard the C-130 [*Bates et al.*, this issue] we will present here only a selection of the most relevant sulfuric acid measurements [*Eisele and Tanner,* 1993].

These measurements near Tasmania revealed that production of new particles were readily occurring in the vicinity of clouds. Data were carefully screened for possible artifact counts caused by the shattering of cloud droplets on the inlet probe that can give rise to spurious high particle counts [*Hudson,* 1993; *Clarke et al.*, 1997]. This did occur at times aboard the C-130 and to differing degrees for the various sample inlets. However, these events were not frequent and could be identified through comparison to C-130 wing probe FSSP data (cloud droplets) in conjunction with RCN concentrations and considerations of relative humidity (RH).

An example of this behavior and the difference between regions of real and artifact high UF concentrations is illustrated in Figures 2a and 2b. The flight altitude and FSSP liquid water content (LWC) provide an indication of the presence of cloud droplets (Figure 2a) that can be compared to the occasions of spurious particle counts caused by cloud droplet shatter (Figure 2b). This clearly reveals periods of cloud penetration when LWC values exceed the background of about 0.02 g kg^{-1}. The fact that during these periods (e.g., near 11.3 hours) the heated CN increase along with total CN reveals that a soluble refractory constituent such as sea salt must have been present to generate small refractory aerosol by shattering of saline droplets [*Clarke et al.*, 1997]. This behavior should be contrasted to the data at 1800 m where we fly out of a region of elevated LWC to a cloud free area (~12.2-12.4 hours). This region of highest UF and UCN counts has no significant LWC and no indication of elevated refractory nuclei. This is a region of recent nucleation in contrast to the in-cloud droplet shatter region. Generally, most data periods were free of droplet shatter artifacts, and often flights through cloud with measurable LWC would not result in elevated particle counts in our sampling system [Weber, unpublished manuscript, 1997].

On November 28, 1995, we deliberately investigated a cloudy region to the west of Tasmania and behind a recent frontal passage. Infrared imagery from the advanced very high resolution radiometer (AVHRR) (Figure 3a) reveals the general conditions and the aircraft track for flight 17 along with times near the vertical profiles to be discussed later. Winds are from the west and turning to SW in the vicinity of Tasmania. A clear region of postfrontal subsidence is evident off the west coast of Tasmania behind the large cloud band moving to the southeast and ahead of a region of broken cumulus convection to the west where clouds typically had bases near 1.5 km and tops about 3.8 km. The flight pattern for this mission is shown in Figure 3b. A picture of the kind of cloud encountered in the area is shown in Figure 4 and indicates one of the more developed anvil topped cumulus rising well above the small cumulus below and detraining into clear air aloft.

A time series for a cloud-outflow C-130 flight on November 18 is shown in Figure 5. The altitude and water vapor mixing

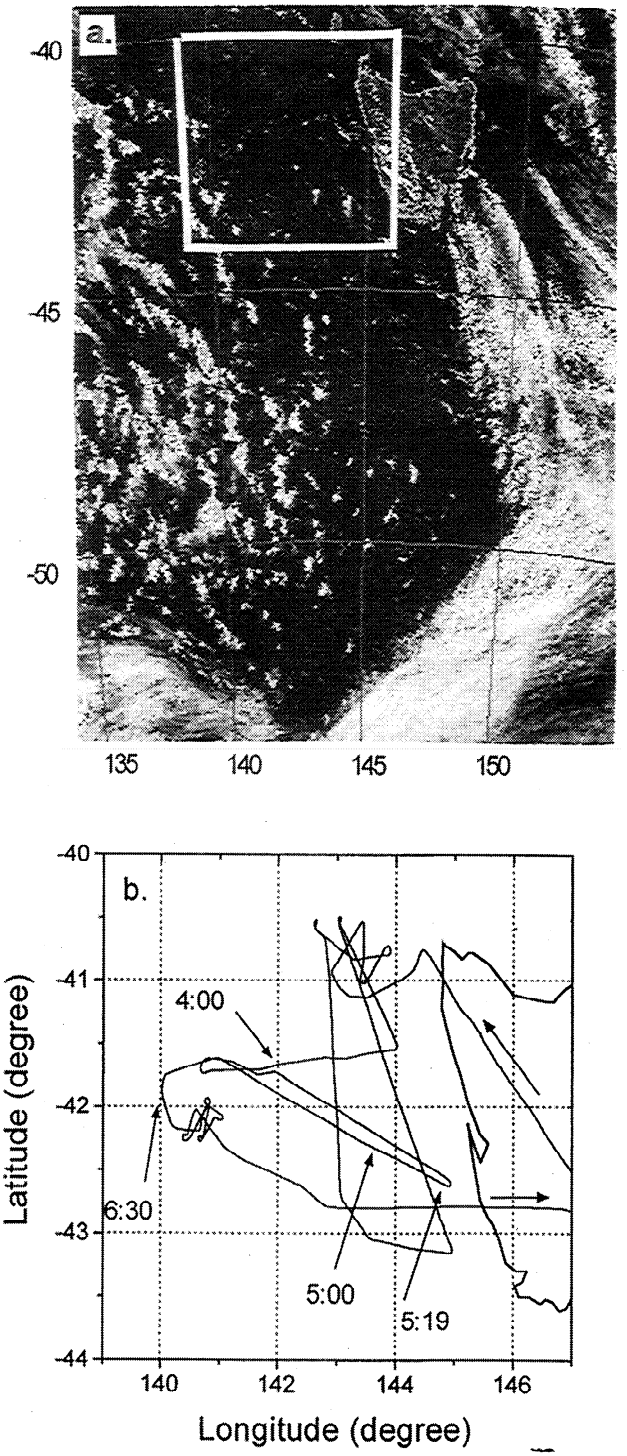

Figure 3. AVHRR IR visible image of (a) cloud field and (b) flight track for November 28, 1995. Locations at 0400 and 0630 are in convective cloudy region, while 0500 and 0519 are in a clear postfrontal subsidence region.

ratio (Figure 5a) and the number concentration of UCN (Dp>3 nm) and UF(3<Dp<10 nm) are shown (Figure 5b) for a range of altitudes from near the surface to about 6 km. Small peaks in UF are encountered sporadically early in the flight but increase markedly in concentration and frequency later in the flight and in cloud outflow regions near 3 km (0600-0800 UTC). Concentrations are generally seen to be highest (2000-4000 cm^{-3})

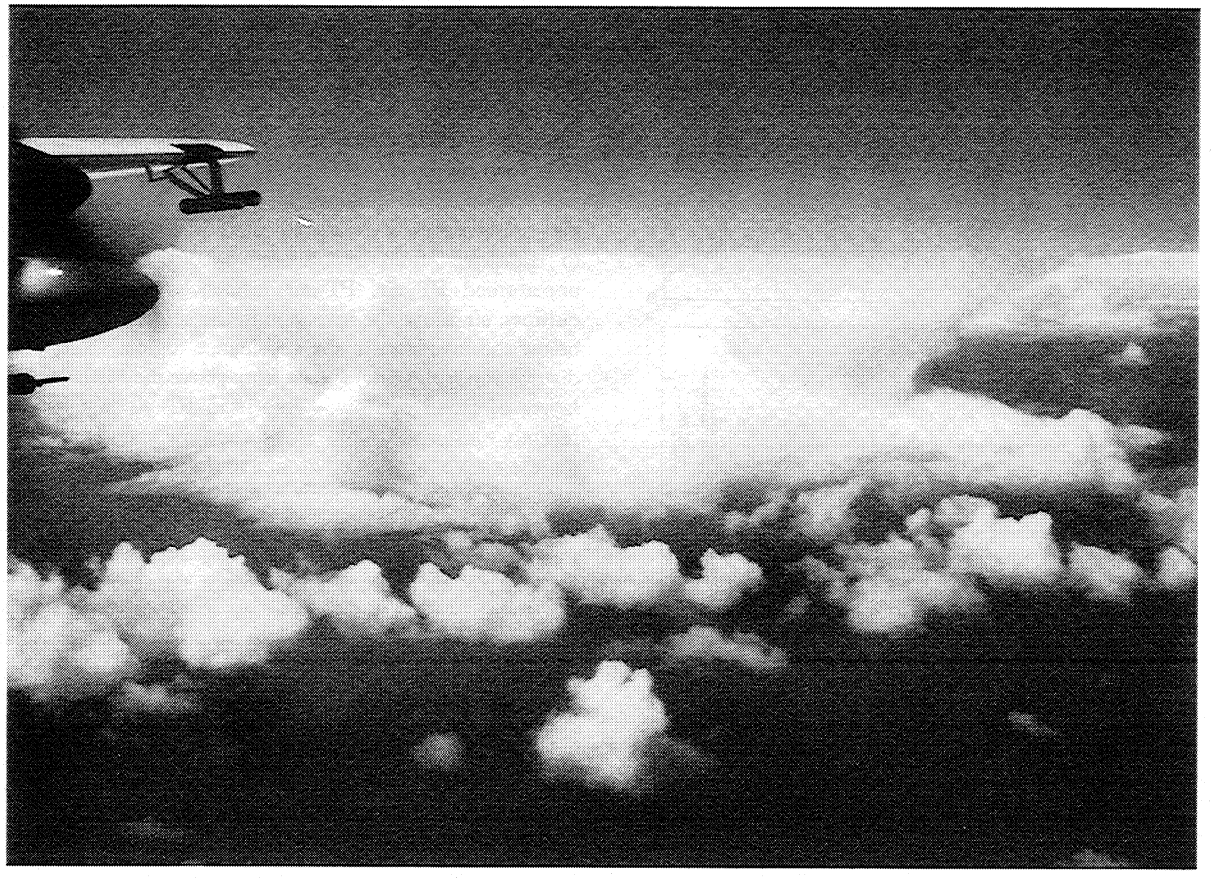

Figure 4. Picture of typical larger cloud outflow top at about 3 km rising above field of smaller lower clouds near 1 km.

in regions where water vapor mixing ratios are intermediate between high near-surface values and the lowest values seen at highest altitudes. This indicates that formation is favored in the mixture of cloud-pumped surface air and dry air aloft that is characteristic of outflow regions. Measurements in cloud, as evident in high RH (not shown) but where droplet shatter did not occur (~0530), have concentrations actually somewhat lower than surface layer values (e.g. 0500), presumably due to in cloud scavenging, while at the edges of this cloud the concentrations of UF increase significantly (~0520 and 0540).

Figure 6 shows vertical profiles of UF, CN, and water vapor mixing ratio profiles (P1, P2, P3) shown in Figure 5a. Each profile reveals layers of pronounced increases in small particle concentrations above the inversion and near regions where the water vapor mixing ratio has a range of values intermediate between MBL values and the lowest values above these layers. Low UF concentrations in the MBL and above these outflow layers confirm that neither region is a source region for these observed high concentrations. The profile in the vicinity of the deepest convective clouds near the end of the day reveals a thick region of UF and CN above the inversion between 2 and 4 km that are a factor of 10 greater than near-surface concentrations. Both this and the earlier profile at 0430-0450 were obtained in the broken convective cloud region (Figure 3a) and exhibit high nuclei concentrations up to 3.5-3.8 km, whereas the profile at 0518-0530 has high concentrations only up to 2.7 km. These lower altitude layers in this cloud free region may reflect the effect of postfrontal subsidence bringing down layers previously formed at higher altitudes. Both in this region and in the region of stronger convection at 0648-0703 the lowest layers with elevated UF concentrations extend almost to the inversion near 1.5 km where they can eventually be entrained into the MBL.

RDMA dry (RH ~20%) particle number distributions for four altitude regions are shown in Figure 7 for this last profile. These are shown for the highest dry layer at 4208 m, the peak layer concentration near 3050 m, in a lower region near 2740 m, and below the inversion near 1520 m. The 4208 m example is representative of all higher altitude drier regions on flight 17 (Figures 5 and 6) and the absence of UF and low water vapor mixing ratio indicates that the highest altitude air mass is not influenced by lower level air and probably has a different history. The lowest near-surface distribution at 1520 m has few particles smaller than 0.02 μm and a relatively large number for sizes greater than 0.08 μm, reflecting where the most mass resides for these distributions. The relative depletion of number near 0.06 μm is evident at 1520 m and is also related to MBL cloud processes discussed below. The 3050 m distribution is in the peak of the cloud outflow UF concentrations (Figure 6c) and reveals a new number peak mode with a maximum at the lower limit of the RDMA channels near 0.01 mm. Since all small particle losses have not been characterized or applied for this system at the smallest sizes, this peak is estimated to be at least

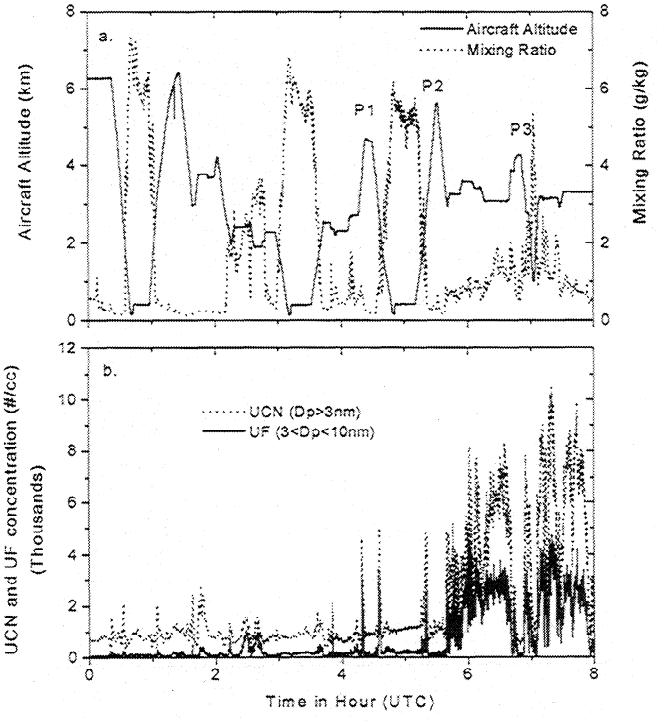

Figure 5. Time series for flight shown in Figure 3 showing (a) aircraft altitude and water vapor mixing ratio and (b) UCN and UF concentrations. Highest UCN and UF are present at altitudes where mixing ratios are intermediate between high values in the MBL and low values aloft, indicative of cloud processed air. Three profiles discussed in text are indicated as (P1, P2, P3).

25% larger than indicated. The distribution at 2740 m shows a similar small particle peak grown to somewhat larger sizes. The FT Aitken mode near 0.035 μm is evident at similar concentrations at all three lower altitudes.

Examples of number distributions from this flight for two different locations and times (Figure 3b) are shown in Figure 8a. These distributions and those of corresponding surface area (Figure 8b) and volume (Figure 8c) are obtained by combining the size distributions collected by the RDMA with distributions from the OPC. In the format provided, the area under the illustrated curves is proportional to the total aerosol number, area, and volume in the Figures 8a, 8b, and 8c, respectively. These data are averaged over the indicated time periods and are chosen to illustrate four representative distributions. These are unperturbed FT air, FT air influenced by convective cloud outflow, air above the inversion in the subsidence region, and air below the inversion in the subsidence region. The FT number distribution (solid line) is data from above the MBL but below the layers of cloud outflow. This is in FT air that has not been recently influenced by cloud outflow and appears to be representative of the environment into which the clouds are detraining. The distribution is monomodal with a number peak diameter near 0.032 μm. There is no evidence of the number minimum near about 0.06-0.1 μm (e.g. Figure 7d) often found in air that has cycled through nonprecipitating clouds [*Hoppel et. al.,* 1986] and characteristic of most remote MBL distributions [*Covert et al.,* 1996; *Clarke et al.,* 1996]. The distribution representative of the outflow region of the clouds (dashed line) has a narrow "nucleation" mode peak at about 0.012 μm superimposed upon the characteristic monomodal FT "background" distribution. These new particles will increase their diameter most rapidly during condensational growth compared to the larger aerosol under the same conditions [*Pruppacher and Klett,* 1989]. The values for water vapor mixing ratios in these cloud outflow regions are also intermediate between those of the MBL and FT, as would be expected for mixed air.

In the post-frontal subsidence region the distribution above the MBL (solid gray line) at 2220 m reveals few particles near the lower limit of the RDMA compared to the outflow region but a

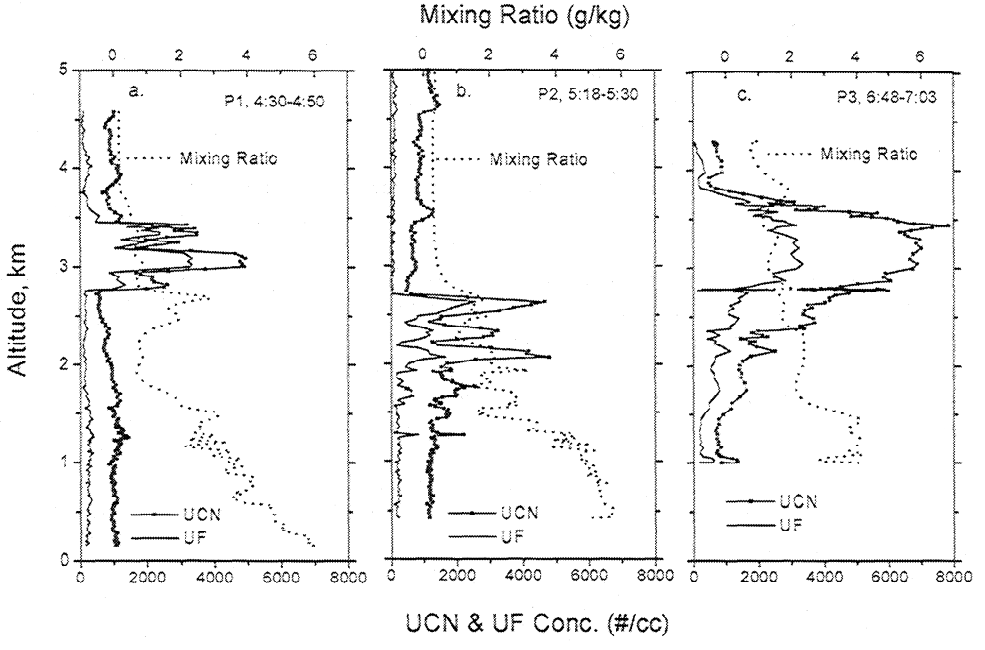

Figure 6. Three profiles (P1, P2, P3) of UCN, UF, and mixing ratios indicated in the time series in Figure 5a. Large increases in UCN and UF are evident aloft and in regions where mixing ratios suggest outflow of MBL air pumped up by clouds. Outflow altitudes are lower in region of post-frontal subsidence (Figure 6b).

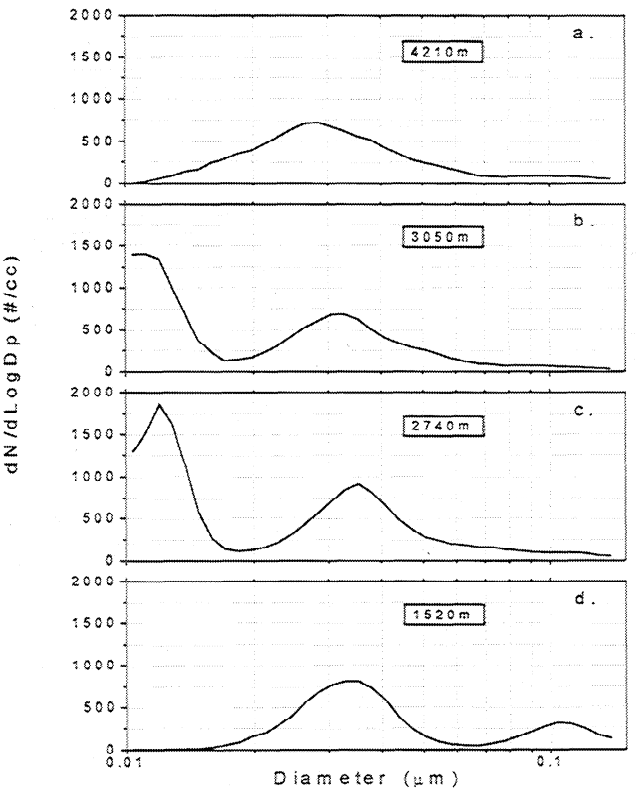

Figure 7. RDMA number distributions for descent profile "P3" illustrated in Figure 6c. Middle panels at intermediate altitudes show clear enhancement of recently formed nuclei in 0.010-0.015 μm range.

broad distribution of nuclei with sizes between about 0.011 μm and the persistent peak in the FT mode near 0.035 μm. The pronounced minima present between nuclei and Aitken modes evident in the outflow regions appears to have been "filled in," presumably by the evolution of the nuclei mode. The distribution below the inversion at 410 m in this subsidence region (dotted line) has even fewer particles at smaller sizes below about 0.013 μm but a mode at 0.020 μm is clearly present upon the lower shoulder of the MBL Aitken mode still centered near 0.035 μm. This feature is also present in shipboard data for this period [*Bates et al.*, this issue]. These particles near 0.020 μm are larger than those observed near cloud outflow and are not present in the "background" case aloft. There was no evidence in our data of new nuclei (less than 0.01 μm) present previously in the MBL nor the more extensive ship data [*Bates et al.*, this issue], suggesting that the origin of this mode was from aloft. Note that the number for this mode present in the MBL is significant (Figure 8a), while their contribution to surface area and mass in the MBL is negligible. The presence of a cloud processed "Hoppel" minima [*Hoppel et al.*, 1986] as well as increased concentrations of the larger MBL aerosol sized by the RDMA in this subsidence region is also evidence of cloud processing. The far greater surface area and volume present in this aerosol is clearly evident in Figures 8b and 8c.

The amplitude of the nuclei modes discussed here and shown in Figure 8a is variable, as might be expected for the large differences in outflow concentrations evident in Figure 6, but the evolution in size is the key point that we emphasize here. This evolution suggests that nucleation in the outflow region is followed by growth and coagulation during subsidence toward the inversion. Upon mixing into the MBL this process increases rapidly, presumably due to exposure to a stronger surface source of gaseous precursors, until these nuclei are incorporated into the MBL Aitken mode. The appearance of these smaller nuclei in regions of high pressure [*Covert et al.*, 1996] and post-frontal subsidence [*Bates et al.*, this issue] is a frequent observation in shipboard data, suggesting that this process is a common event for these midlatitude regions. The volume distributions (Figure 8c) include the OPC size distributions for the larger aerosol and reveal the clear increase in mass associated with the larger particle sizes observed in the MBL. In many locations this contributes to a pronounced submicrometer sulfate peak near 0.3 μm in response to gas phase fluxes from the surface that can support heterogeneous gas to particle conversion. However, in this postfrontal well scavenged air most of the large particle volume in Figure 8c in the MBL is sea salt. All of these observations are consistent with the notion that this aerosol represents a mix between a typical MBL aerosol with a cloud processed minima and recently nucleated aerosol from above that have grown during subsidence and mixing into the MBL.

4. Photochemical Production

A specific flight mission was carried out in order to test our expectation that the new nuclei observed in the vicinity of clouds were photochemically produced. In order to do this we required

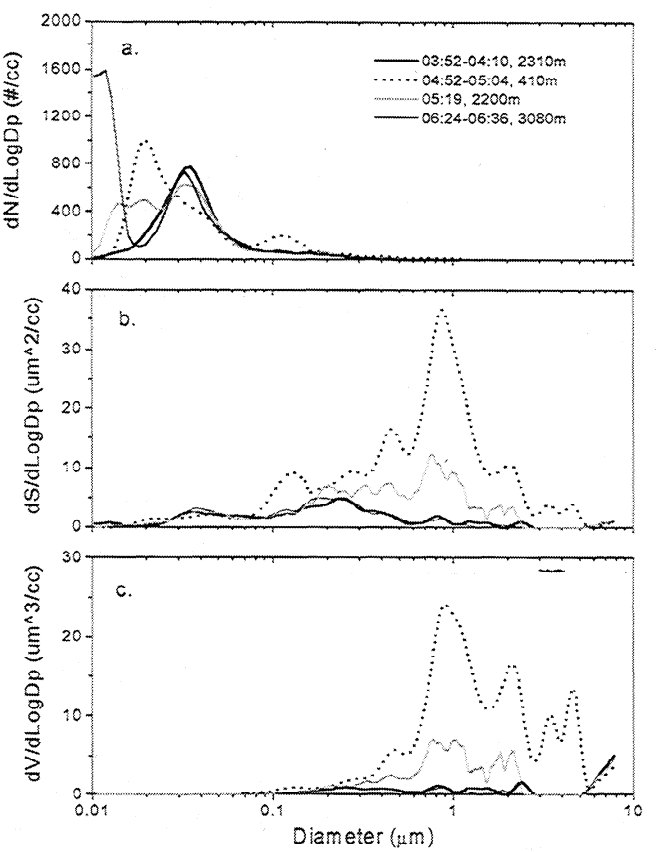

Figure 8. (a) Aerosol number, (b) surface, and (c) volume for cases selected from convective and postfrontal subsidence regions indicated in Figure 3. Unperturbed FT aerosol in convective region (heavy solid line), mixed FT outflow from convective region (thin solid line), postfrontal subsidence above inversion (heavy gray line), and postfrontal MBL below inversion (dotted line). See text for details.

sampling of similar cloud outflow early in the morning before the onset of active photochemistry and then later after gaseous precursors and reaction products had time to accumulate. For unambiguous interpretation, this needed to be done in a region of clean air that had not had an opportunity for recent particle production through cloud outflow in the previous day or more. The region also had to be within range of our base in Hobart in order to be able to make repeat measurements at the same location separated by several hours.

An ideal situation presented itself on December 10 during Flight 27. Clean air from the Southern Ocean was being advected toward Tasmania from the ESE. The IR satellite imagery revealed an extensive field of cumulus clouds were embedded in this flow for distances upwind of about 1000 km. These had cloud tops generally less than 2 km but within about 200 km of the west coast of Tasmania colder IR cloud top temperatures indicated isolated cumulus tops increased to about 3 km altitude. This meant that deeper convection and associated cloud outflow was occurring near and into regions of previously unperturbed air. The mission consisted of making measurements in the outflow regions and the vicinity of these larger developed cumulus in the early morning and then returning to the same region later in the day in order to determine whether particle production was enhanced after sustained active photochemistry. Selection of the region to be returned to was based upon the estimated trajectory of the cloudy air for the wind speeds and directions measured on the morning flight.

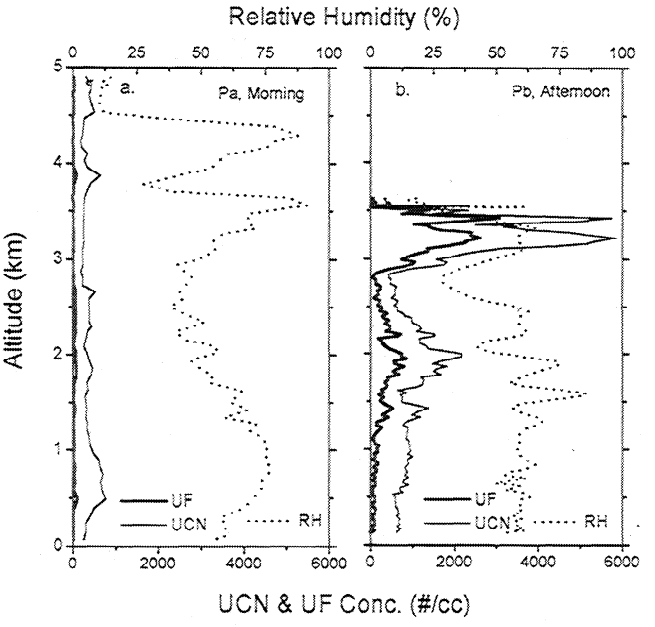

Figure 10. Vertical profiles of UCN, UF, and RH near (a) morning (Pa) and (b) afternoon (Pb) cloud outflow regions shown in Figure 9. Although the morning profile shows high RH layers aloft indicative of outflow, the UCN and UF concentrations remain low. Similar elevated RH layers aloft in afternoon reveal large enhancements in UCN and UF above the MBL.

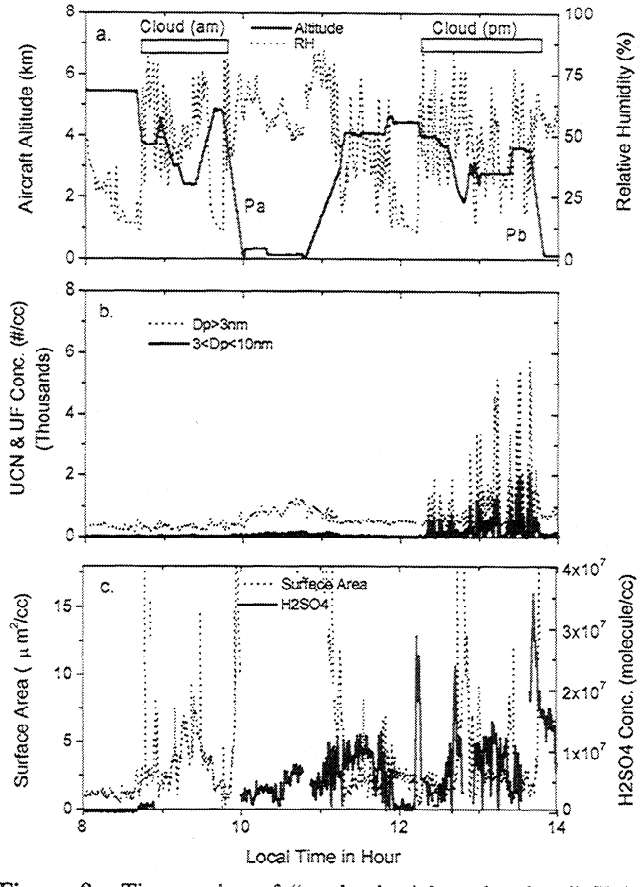

Figure 9. Time series of "nucleation/photochemistry" flight looking at cloud outflow in early morning and afternoon showing (a) aircraft altitude and RH with cloud regions and associated profiles indicated, (b) UCN and UF, and (c) aerosol surface area and sulfuric acid gas concentration.

A time series for key parameters for this flight including altitude CN, UF, H_2SO_4 gas, surface area, and RH are shown in Figure 9. The periods for the morning cloud passes, the excursion to Cape Grim for intercomparisons, and the afternoon cloud passes are indicated. Morning measurements above, below, and in the outflow region were made near 0900 local standard time (LST) but with no evidence of new UF particle production present that exceeded flow uncertainties for the difference measurement (5-10%). A small increase in H_2SO_4 near 0845 is evident before the instrument stopped working until it was brought back on line at 1000. In spite of this missing data the H_2SO_4 during the boundary layer leg for 1000-1100 LST starts out relatively low and well below the MBL concentrations observed later near 1400 LST suggesting that it would have continued to be low for the period of missing data. At 0930 LST we left this cloudy region to carry out other instrument comparisons at Cape Grim and did not return until about 1200 LST. Repeated sampling around the cloud region and outflow between 1230 and 0130 LST clearly show dramatic increases in the UF concentrations of several thousand per cubic centimeter between 2500 and 3500 m. This is consistent with the previous observations in regions of high UF and demonstrate that the production of new particles is linked to photochemical processes that involve the production of sulfuric acid gas. The horizontal leg centered around 1430 represents our attempt to stay in an outflow layer as we returned toward Hobart. This is often difficult since the layers can be thin and finite as well as sloped along potential temperature surfaces.

The vertical profiles taken in the vicinity of the morning and afternoon cloud comparison legs are compared in Figure 10. The influence of lower level clouds is primarily below 2 km and the deeper convective clouds above that altitude. In the morning, total UCN are between 200 and 600 cm^{-3} with highest concentration in the moist layer below 1 km. Corresponding UF

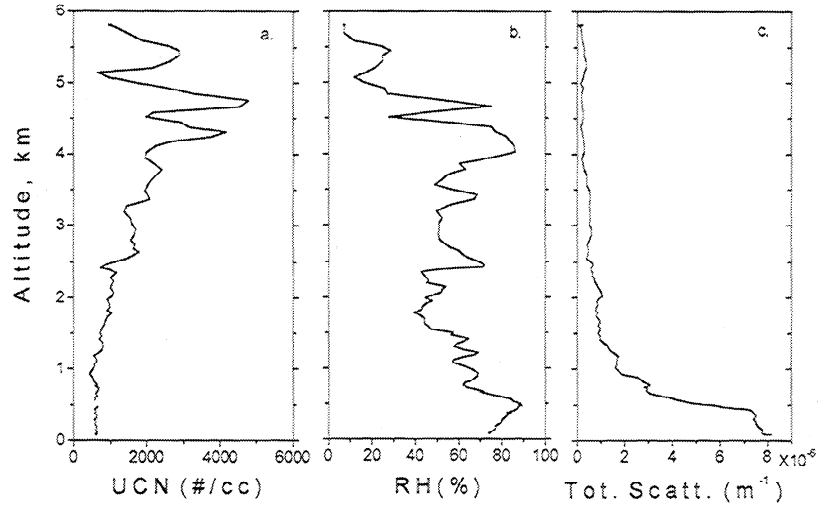

Figure 11. Profiles of (a) UCN, (b) RH, and (c) aerosol light scattering (fast response index for surface area) for an equatorial descent profile near Christmas Island. Elevated UCN aloft are clearly related to elevated RH and overall concentration gradient from aloft toward the surface. Peak concentrations are also observed in regions of lowest scattering coefficient (surface area).

particles remain low throughout the column up to 5 km. This is true even at 3.5 and 4.4 km where high RH indicates cloud outflow air. When we return to this same region later in the afternoon, the profile shows similar concentrations below 1 km but marked increases in UCN and UF particles in the regions where increased RH implies cloud processed air for both lower clouds and the upper clouds detraining near 3.0-3.5 km.

5. Equatorial Observations

Although ACE 1 focused on experiments in the Southern Ocean near Tasmania, some data were collected during transect flights to and from this region. It is of interest to compare the midlatitude observations above with data from the equatorial region, since it was there that we first observed elevated UF concentrations aloft [*Clarke,* 1993] and where we later found evidence for entrainment of new particles into the MBL [*Clarke et al.,* 1996]. This region is also of interest because it differs from the midlatitude Tasmania region with its active frontal systems. Here the narrow band of deep convection in the Intertropical Convergence Zone (ITCZ) is fed by generally stable low level trade wind surface flows capped by a subsidence inversion. The more stable meteorology and large scale homogeneity with the absence of frontal systems provides for a simpler system for investigating aerosol evolution.

Figures 11a, 11b, and 11c show vertical profiles of UCN particle concentrations, RH, and the aerosol scattering coefficient collected in the vicinity of Christmas Island and located south of the ITCZ in the equatorial Pacific (1°N, 158°W). These elevated number concentrations extend up to about 6 km and much higher than for the Tasmania region, presumably a result of the more intense convection present in the nearby ITCZ. Even higher concentrations near ITCZ convection were observed previously up to 8 km altitude [*Clarke,* 1993]. Also shown is the scattering coefficient (Figure 11c) since FSSP derived surface area was not available for this flight. The dry scattering coefficient provides a relative index for the variability in aerosol surface area. The data are consistent with our Tasmania data and earlier observations [*Clarke,* 1993] in that the highest particle concentrations are generally present in regions of lowest aerosol surface area. These low scattering coefficients are also indicative of clean background air that is well scavenged of most continental and MBL aerosol mass.

Although the profile in Figure 11 was not specifically taken in the vicinity of cloud outflow, the correspondence between higher altitude particle concentrations and RH evident above about 2 km is indicative of cloud processed air. However, in this region few particles were observed with sizes below about 0.010 μm indicating that the aerosol is more aged than that shown for Tasmania (Figures 6 and 7). This is also evident in the RDMA size distributions taken at various altitudes during the descent and shown in Figure 12a and 12b. These show distributions at 12 altitudes and divided into two panels for clarity. Particle concentrations for the upper altitudes are in the 2000-4000 cm^{-3} range but are for sizes somewhat larger than those seen near outflow regions around Tasmania (Figure 8). However, there is a clear shift to larger particle sizes with decreasing altitude. This shift continues steadily while descending toward the MBL, and the distribution in the MBL is very close to that we have reported in an earlier paper for longer term surface measurements [*Clarke et al.,* 1996]. Moreover, the distribution shown for just above the MBL (Figure 12b, 1983 m) is the monomodal distribution predicted to exist above the MBL and needed to support the argument for entrainment from aloft also presented in that paper. This distribution has also been predicted from model results with a similar formation scenario [*Raes,* 1995]. The steady change in the distribution below 2 km shows the gradual increase in larger sizes and decrease in smaller sizes as the surface is approached. This would be expected for processing through nonprecipitating MBL clouds that favor heterogeneous chemistry and addition of mass to those nuclei activated in cloud [*Hoppel et al., 1986*]. This results in growth of some of these nuclei into the larger MBL accumulation mode and creation of a "Hoppel" minimum near 0.09 μm, as seen in the MBL distribution shown in Figure 12b.

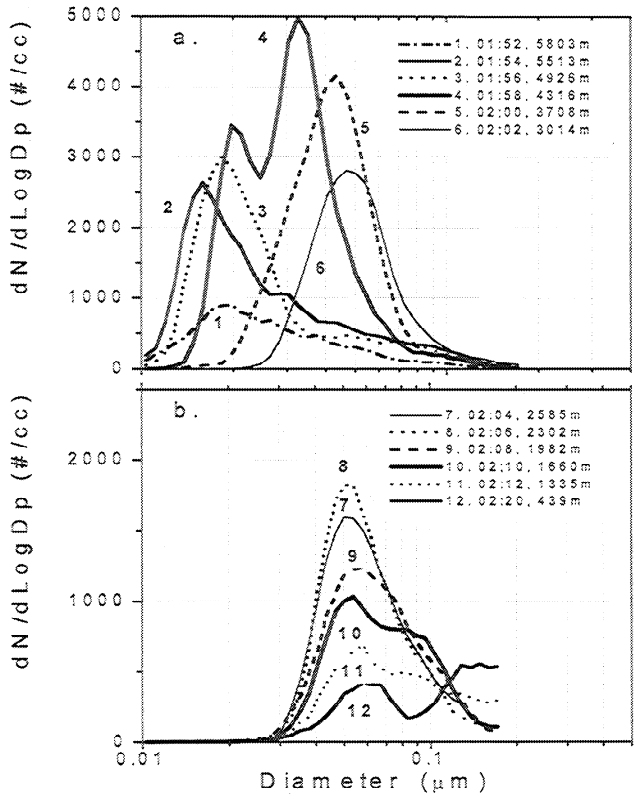

Figure 12. Individual plots of the RDMA number distributions for the 12 altitudes indicated in Figure 11. Two panels are shown with different vertical scales for clarity. A clear and consistent trend of increasing size and decreasing concentration is evident during the descent. Near the surface a transition from monomodal to bimodal is evident and indicative of heterogeneous gas to particle conversion on cloud nuclei in the MBL

6. Surface Area

As mentioned earlier, surface area appears to be a key parameter that affects the production of new particles under the conditions we have described. Suggestion of the critical range of values that exist when nucleation is favored can be seen by plotting the nuclei concentration as a function of FSSP ambient surface area for flights 17 and 23 that exhibited a range of conditions that included nucleation events in cloud outflow. These are shown in Figures 13a and 13b for November 28 and Figures 13d and 13e for December 7 for both the total UCN and the UF concentrations, respectively. Also included are corresponding plots of the relative humidity in Figures 13c and 13f which tended to be near 60-80% in the MBL and about 10-20% in FT unperturbed by recent cloud outflow. The subset of smaller UF nuclei have been corrected for pressure dependent flow effects observed in the TSI 3010 CN counter. For surface areas above about 20 μm cm^{-3} the UF values vary about zero but are within the flow uncertainty of the difference measurement of the two nuclei counters used to establish their concentration.

The November 23 flight tended to be at higher altitudes in outflow near 3.5 km and in generally lower humidity air than the December 7 flight that was more typical of 2.5 km. In regions of moderate surface area (>20 μm^2 cm^{-3}) on this flight we see generally low and steady UCN and UF concentrations and RH values typically of either MBL or FT values. The peaks in UCN and UF are for FSSP surface areas between 5 and 10 μm^2 cm^{-3}. Surface areas below this show typical low counts, but comparison with the corresponding RH data reveals that this is dry FT air not influenced by cloud. The high density of data points in elevated UF correspond to the high density of RH values that lie between 20-40%. This represents air that is a mix of MBL and FT air, as would be expected for cloud outflow regions. UF concentrations are about 40% of UCN concentrations and indicating a large fraction of UCN are in the UF size range.

Similar behavior is evident for the December 7 flight, although RH values are significantly higher, and more humid FT air is evident for the lower altitudes represented. UCN and UF concentrations are lower for this case but are distributed over a somewhat greater range of FSSP surface areas up to 20 μm cm^{-3} and for higher RH values in the 50-80% range. The fraction of UCN in the UF size range is less than 20%, revealing that recently nucleated particles had grown larger for this case. This would be consistent with nucleation in lower altitude cloud outflow mixed with MBL air having both higher RH and surface area as well as possibly higher gaseous precursors for GPC than the November 23 case.

These observations, coupled with the observation that no new UF are observed in cloud interiors, imply that new UF are only likely to be produced in the vicinity of cloud outflow when FSSP

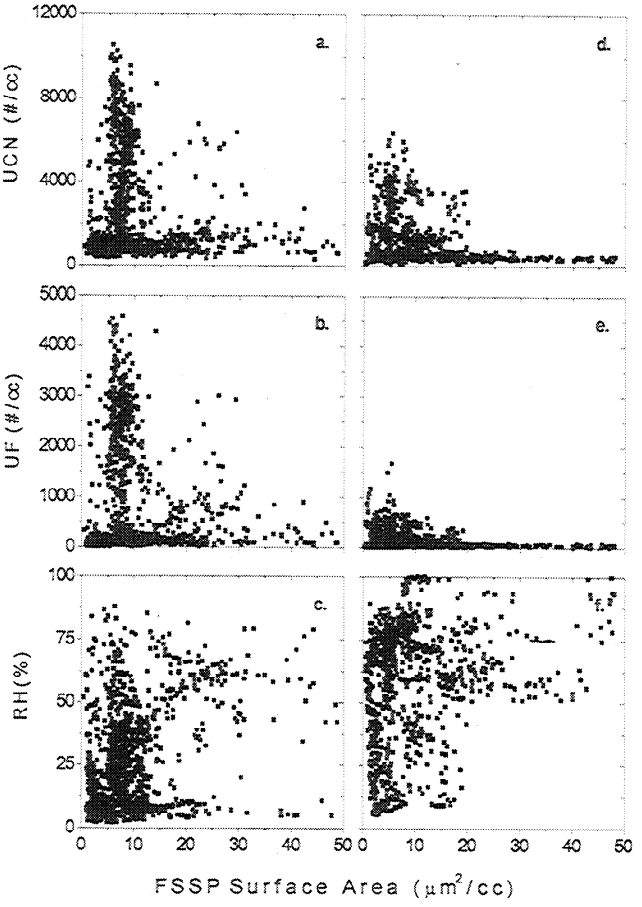

Figure 13. An example of the relation of elevated (a) UCN, (b) UF, and RH to FSSP surface area for the data collected on Flight 23. Air with evidence for recent nucleation events are only evident for FSSP surface areas below 20 mm^2 cm^{-3}. Because UF are defined by a difference between instruments, small differences in flows, response time, etc. can be seen to yield negative concentrations.

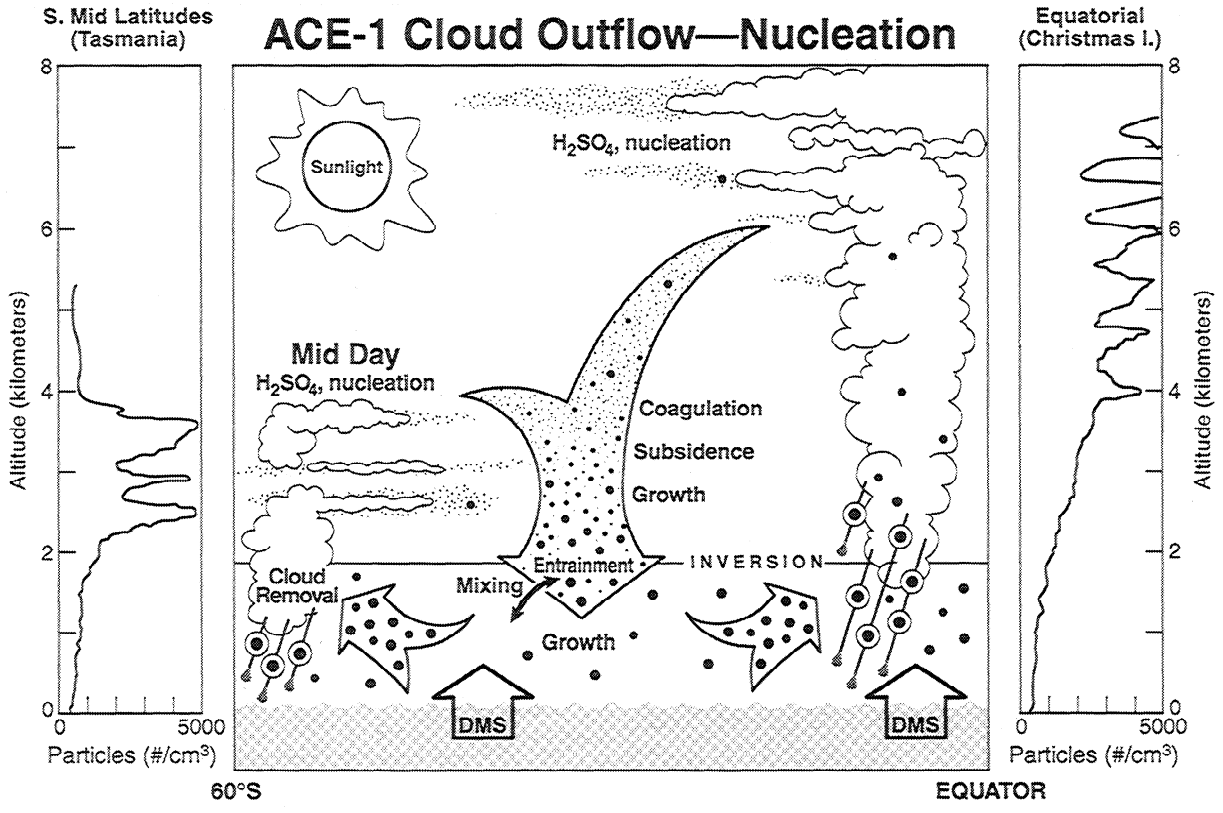

Figure 14. A cartoon of the nucleation and cycling of particles in the remote marine troposphere as evidence from the observations made on ACE 1. Clouds both scavenge MBL aerosol and source new particles aloft with meteorology and subsidence linking these mechanisms over large spatial scales (see text).

surface areas are below about 5 μm^2 cm^{-3}. Separate evidence for new particle formation in the 3-4 nm range was also directly observed in these regions (P. H. McMurry, personal correspondence, 1997). The fact that the larger UCN have concentrations higher than the UF in most of these regions suggests that growth of nuclei up to 10 μm diameter or larger must occur in a relatively short period (tens of minutes to hours) as the cloud outflow mixes with dry clean air. We note that for these regions of FSSP surface area that are near or below this value, an appreciable contribution to total surface area exists for particle sizes below our "FSSP" lower threshold. Examination of typical RDMA data under these conditions suggest that an additional 50-100% of the FSSP surface area may be present below our FSSP detection limit. During these periods of recent "nucleation events" some of this is new surface area, at times 30%, that results from the nucleation itself. At the same time some of the surface area must be a result of mixing with the environmental air after the onset of nucleation. Hence, we estimate the actual surface area at time of nucleation lies somewhere between the FSSP value and about twice that value.

7. Conclusions

Several flights have been described from the ACE 1 experiment that were focused on aerosol nucleation in the free troposphere. All of these observations were found to be linked directly or by inference to the air that had been recently processed by clouds. The process of nucleation appeared to be active in the region of detrainment and mixing described as cloud outflow and that growth to detectable sizes of 0.003 μm appeared to be rapid at perhaps a few tens of minutes to hours. Sulfuric acid concentrations also appeared moderately enhanced in these regions with typical concentrations of the order of 10^7 molecules cm^{-3}. Both particle production and sulfuric acid were found to be more enhanced in cloud outflow regions in noon to early afternoon, apparently as a result of more active photochemistry. Highest new particle concentrations were generally associated with regions of lowest surface areas and water vapor mixing ratios intermediate between moist surface layers and dry regions aloft and above cloud. These observations are in general agreement with previous observations [*Perry and Hobbs,* 1994] and support their description of cloud processing, although we note that our midlatitude observations occurred at significantly lower altitudes and warmer temperatures(i.e., -2° to -15°C).

Growth and evolution of these particles aloft was evident in the data over periods estimated to be hours to a day or so during which time the smaller nuclei appeared to merge with an Aitken mode usually centered near 0.035-0.060 μm depending upon location and altitude. Flights in postfrontal subsidence revealed smaller nuclei in the MBL both aboard the C-130 and the R/V *Discoverer* [*Bates et al.,* this issue], indicating that these were likely to have been mixed into the MBL as particles formed aloft by previous convective clouds.

Observations in the tropical free troposphere near Christmas Island supported earlier data that suggested convective cloud processes near the ITCZ resulted in new particle production aloft.

Vertical profiles in this region revealed that smallest monomodal nuclei were present aloft that gradually increased in

size during descent toward the MBL. These data support the hypothesis that subsidence and entrainment from aloft provided a monomodal nuclei source with a number mean diameter near 0.06 μm that can replenish the equatorial MBL aerosol against intermittent removal process (e.g., precipitation, coagulation, etc.).

Together, the results from both of these regions suggest an aerosol life cycle for the remote MBL that is coupled to cloud processes, subsidence and entrainment from the free troposphere. This is illustrated schematically here in Figure 14. In both midlatitude and equatorial regions, clouds play a role in scavenging larger activated aerosol through precipitation and thereby reducing aerosol surface area prior to mixing with the drier free troposphere air. In doing so they pump reactive gases aloft and water vapor into a cooler environment with often enhanced actinic flux from both direct and diffusely reflected radiation. These processes appear to result in enhanced production of sulfuric acid gas that can result in rapid homogeneous nucleation of new particles that continue to grow and evolve through heterogeneous processes. In the midlatitude conditions near Tasmania this process occurred at altitudes from about 2-3.5 km such that active subsidence could soon bring newly formed particles close to the inversion where they could be entrained into the MBL before they had been assimilated into the ubiquitous Aitken mode. In equatorial conditions the deeper convection resulted in particle formation at generally higher altitudes. This suggests that a longer aging, transport, and evolution is expected before the moderate subsidence rates for the region bring them near enough to the MBL to be entrained. This results in a more stable and well aged monomodal aerosol above the tropical MBL that can be entrained into it and sustain the relatively stable and larger Aitken mode encountered in these regions [*Clarke et al.*, 1996; *Covert et al.*, 1996].

Hence clouds both scavenge the MBL aerosol possessing most aerosol mass and surface area but pump reactive gases aloft where photochemical production of sulfuric acid occurs and nucleation of new UF particles results. After evolution over a period of time that varies with regions and conditions, many of these subside to the MBL where they grow by heterogeneous gas to particle conversion. This suggests the MBL aerosol represents a dynamic equilibria between entrained aerosol, surface-produced sea salt, heterogeneous GPC in the MBL, and episodic removal by clouds. In this fashion the MBL aerosol number, surface, and mass distributions can be maintained in a quasi steady state through a cycle that is intimately coupled to the clouds that have their roots in the MBL and tops in the free troposphere.

Acknowledgments. This research is a contribution to the International Global Atmospheric Chemistry (IGAC) Core project of the International GeosphereBiosphere Programme (IGBP) and is part of the IGAC Aerosol Characterization Experiments (ACE). Special thanks is also extended to D. Baumgardner for FSSP aerosol surface area data provided by NCAR. Support was provided through NSF Atmospheric Chemistry under grant ATM-9419475 and NASA NAGW3766. This is SOEST Publication 4531.

References

Anderson, T. L., et al., Performance characteristics of a high-sensitivity, three-wavelength, total scatter/backscatter nephelometer, *J. Atmos. Oceanic Tech.*, no. 1, 1996.

Andreae, M. O., and H. Raemdonck, Dimethyl sulfide in the surface ocean and marine atmosphere: A global view, *Science, 2,* 744-747, 1983.

Ayers, G. P., J. P. Ivey, and R. W. Gillet, Coherence between seasonal cycles of dimethyl sulfide, methane sulfonate, and sulphate in marine air, *Nature, 349,* 404-406, 1991.

Bates, T. S., A. D. Clarke, V. N. Kapustin, J. E. Johnson, and R. J. Charlson, Oceanic dimethyl sulfide and marine aerosol: Difficulties associated with assessing their covariance, *Global Biogeochem. Cycles, 3,* 299-304, 1989.

Bates, T. S., R. P. Kiene, G. V. Wolfe, P. A. Matrai, F. P. Chavez, K. R. Buck, B. W. Blomquist, and R. L. Cuhel, The cycling of sulfur in surface seawater of the northeast Pacific, *J. Geophys. Res., 99,* 7835-7843, 1994.

Bates, T. S., V. N. Kapustin, P. K. Quinn, D. S. Covert, D. J. Coffman, C. Mari, P. A. Durkee, W. De Bruyn, and E. Saltzman, Processes controlling the distribution of aerosol particles in the lower marine boundary layer during ACE 1, *J. Geophys. Res.*, this issue.

Baumgardner, D., and A. Clarke, Changes in aerosol properties with relative humidity in the remote southern hemisphere marine boundary layer, *J. Geophys. Res.*, this issue.

Bonsang, B., B. C. Nguyen, A. Gaudry, and G. Lambert, Sulfate enrichment in marine aerosols owing to biogenic gaseous sulfur compounds, *J. Geophys. Res., 85,* 7410-7416, 1980.

Charlson, R. J., J. E. Lovelock, M. O. Andreae, and S. G. Warren, Oceanic phytoplankton, atmospheric sulfur, cloud albedo, and climate, *Nature, 326,* 655-661, 1987.

Charlson, R. J., S. E. Schwartz, J. M. Hales, R. D. Cess, J. A. Coakely Jr., J. E. Hansen, and D. J. Hofmann, Climate forcing by anthropogenic aerosols, *Science, 255,* 423-430, 1992.

Clarke, A. D., A thermo-optic technique for in-situ analysis of size-resolved aerosol physicochemistry, *Atmos. Environ., Part A, 25* (3/4), 635-644, 1991.

Clarke, A. D., Atmospheric nuclei in the Pacific midtroposphere: Their nature, concentration, and evolution, *J. Geophys. Res., 98,* 20,633-20,647, 1993.

Clarke, A. D., Z. Li, and M. Litchy, Aerosol dynamics in the equatorial Pacific marine boundary layer: Microphysics, diurnal cycles, and entrainment, *Geophys. Res. Lett., 23,* 733-736, 1996.

Clarke, A. D., T. Uehara, and J. N. Porter, Atmospheric nuclei and related aerosol fields over the Atlantic: Clean subsiding air and continental pollution during ASTEX, *J. Geophys. Res., 102,* 25,281-25,292, 1997.

Covert, D. S., V. N. Kapustin, P. K. Quinn, and T. S. Bates, New particle formation in the marine boundary layer, *J. Geophys. Res., 97,* 20,581-20,589, 1992.

Covert, D. S., V. N. Kapustin, T. S. Bates, and P. K. Quinn, Physical properties of marine boundary layer aerosol particles of the mid-Pacific in relation to sources and meteorological transport, *J. Geophys. Res., 101,* 6919-6930, 1996.

Eisele, F. L., and D. J. Tanner, Measurement of the gas phase concentration of H_2SO_4 and methane sulfonic acid and estimates of H_2SO_4 production and loss in the atmosphere, *J. Geophys. Res., 98,* 9001-9010, 1993.

Eisele, F. L., R. L. Mauldin III, D. J. Tanner, J. Fox, T. Mouch, and T. Scully, An inlet/sampling duct for airborne OH and sulfuric acid measurements, *J. Geophys. Res., 102,* 27,993-28,001, 1997.

Gras, J. L., CN, CCN and particle size in Southern Ocean air at Cape Grim, *Atmos. Res., 35,* 233-251, 1995.

Hegg, D. A., L. F. Radke, and P. V. Hobbs, Particle production associated with marine clouds, *J. Geophys. Res., 95,* 13,917-13,926, 1990.

Hoppel, W. A., G. M. Frick, and R. E. Larson, Effect of nonprecipitating clouds on the aerosol size distribution in the marine boundary layer, *Geophys. Res. Lett., 13,* 125-128, 1986.

Hoppel, W. A., G. M. Frick, J. Fitzgerald, and R. E. Larson, Marine boundary layer measurements of new particle formation and the effects nonprecipitating clouds have on aerosol size distributions, *J. Geophys. Res., 99,* 14,443-14,459, 1994.

Hudson, J. G., Cloud condensation nuclei near marine cumulus, *J. Geophys. Res., 98,* 2693-2702, 1993.

Kriedenweiss, S. M., and J. H. Seinfeld, Nucleation of sulfuric acid-water and methanesulfonic acid-water solution particles: Implications for the atmospheric chemistry of organosulfur species, *Atmos. Environ., 22,* 283-296, 1988.

McMurry, P. H., and M. R. Stolzenburg, On the sensitivity of particle size to relative humidity for Los Angeles aerosols, *Atmos. Environ., 23,* 497-507, 1989.

Perry, K. D., and P. V. Hobbs, Further evidence for particle nucleation in clear air adjacent to marine cumulus clouds, *J. Geophys. Res., 99,* 22,803-22,818, 1994.

Pruppacher, H. R., and J. D. Klett, *Microphysics of Clouds and Precipitation,* D. Reidel, Norwell, Mass., 1989.

Raes, F., Entrainment of free-tropospheric aerosol as a regulating

mechanism for cloud condensation nuclei in the remote marine boundary layer, *J. Geophys. Res., 100*, 2893-2903, 1995.

Raes, F., R. Van Dingenen, J. Wilson, and A. Saltelli, Cloud condensation nuclei from dimethyl sulfide in the natural marine boundary layer: Remote vs. in-situ production, in *Dimethyl Sulfide, Ocean, Atmosphere and Climate*, edited by G. Restelli and G. Angeletti, pp. 311-322, Kluwer Acad., Norwell, Mass., 1993.

Russell, L. M., S. N. Pandis, and J. H. Seinfeld, Aerosol production and growth in the marine boundary layer, *J. Geophys. Res., 99*, 20,989-21,004, 1994.

Shaw, G. E., Production of condensation nuclei in clean air by nucleation of H_2SO_4, *Atmos. Environ.*, 23, 2053-2057, 1989.

Weber, R. J., A. D. Clarke, M. Litchy, J. Li, G. Kok, R. D. Schillawski, and P. N. McMurry, Spurious aerosol measurements when sampling from aircraft in the vicinity of clouds, *J. Geophys. Res.* (in press).

Weber, R. J., and P. H. McMurry, Fine particle size distributions at the Mauna Loa Observatory, Hawaii, *J. Geophys. Res., 101*, 14,767-14,775, 1996.

Weber, R. J., P. H. McMurry, F. L. Eisele, and D. J. Tanner, Measurement of expected nucleation precursor species and 3-500 nm diameter particles at Mauna Loa Observatory, Hawaii, *J. Atmos. Sci., 52*, 2242-2257, 1995.

Wiedensohler, A., et al., Intercomparison study of size dependent counting efficiency of 26 condensation particle counters, *Aerosol Sci. Technol.*, in press, 1997.

Zhang, S. H., Y. Akutsu, L. M. Russell, R. C. Flagan, and J. H. Seinfeld, Radial Differential Mobility Analyzer, *Aerosol Sci. Technol., 23*, 357-371, 1995.

A. D. Clarke, M. Litchy, and J. L. Varner, School of Ocean and Earth Science and Technology, University of Hawaii, Honolulu, HI 96822. (e-mail: tclarke@soest.hawaii.edu)

F. Eisele, GTRI, Georgia Institute of Technology, Atlanta, GA 30332. (e-mail: eisele@acd.ucar.edu)

R. L. Mauldin and D. Tanner, ACD, NCAR, Boulder, CO 80303. (e-mail: mauldin@acd.ucar.edu)

(Received July 2, 1997; revised October 7, 1997;
accepted October 16, 1997.)